ELSEVIER

International Journal of Mass Spectrometry 181 (1998) 99–111

International Journal of Mass Spectrometry

Stratospheric chemical ionization mass spectrometry: nitric acid detection by different ion molecule reaction schemes

E. Arijs[a,*], A. Barassin[b], E. Kopp[c], C. Amelynck[a], V. Catoire[b], H.P. Fink[c], C. Guimbaud[b], U. Jenzer[c], D. Labonnette[b], W. Luithardt[c], E. Neefs[a], D. Nevejans[a], N. Schoon[a], A.-M. Van Bavel[a]

[a]*Belgian Institute for Space Aeronomy, Ringlaan 3, B-1180 Brussels, Belgium*
[b]*LPCE-CNRS, 3A, Av. de la Recherche Scientifique, F-45071 Orléans, France*
[c]*Physikalisches Institut, Universität Bern, Sidlerstrasse 5, CH-3012 Bern, Switzerland*

Received 29 June 1998; accepted 28 August 1998

Abstract

Detailed height profiles of stratospheric nitric acid mixing ratios have been derived with a baloon borne chemical ionization mass spectrometer by applying several ion molecule reaction schemes, each associated to a specific and selective ion source. These ions (CO_3^-, Cl_n^-, CF_3O^-, and $CF_3O^-H_2O$) give rise to specific product ions (mainly $CO_3^-HNO_3$, NO_3^-HCl, NO_3^-HF, and $CF_3O^-HNO_3$) upon reaction with ambient nitric acid molecules. This paper reports on the instrumental details as well as on the results obtained during two balloon flights with the instrument. Within the accuracy of the measurements, the nitric acid height profiles obtained with the three different ion sources are in good agreement with one another as well as with literature data. (Int J Mass Spectrom 181 (1998) 99–111) © 1998 Elsevier Science B.V.

Keywords: CIMS; Nitric acid, Stratosphere; Aeronomy

1. Introduction

Nitric acid is formed in the Earth's atmosphere by the three-body reaction

$$NO_2 + OH + M \rightarrow HNO_3 + M \quad (1)$$

M being mainly N_2 and O_2. It is a rather stable molecule with a long photochemical lifetime (in the stratosphere as well as in the troposphere) and it is an important reservoir gas for the reactive nitrogen oxides [1,2]. Apart from the destruction by photolysis and reaction with OH, its loss is controlled by precipitation, either by rainout or dry deposition.

Its formation through reaction (1) leads to a decrease in the NO_x species and thus contributes to the disruption of the catalytic ozone destruction, involving NO and NO_2 [3]. It also plays an important role in ozone depletion processes controlled by aerosol formation and heterogeneous chemistry (such as polar ozone depletion), because its removal by inclusion into aerosols indirectly reduces the NO_2 concentration and thus the formation of $ClONO_2$, through the reaction of ClO with NO_2. As a result, more active chlorine can be made available for the attack of ozone [2].

* Corresponding author: E-mail: etienne.arijs@oma.net

PII S1387-3806(98)14162-3

Several measurements of HNO_3 in the stratosphere have been performed by remote sensing, based upon optical methods [4–7]. However, these optical measurements are mostly limited to some periods of the day (sunset, sunrise) or at least to the availability of sunlight. They require complicated inversion methods and result in average values for the concentrations over long optical paths.

For the study of local phenomena, such as measurements in the arctic stratosphere [8], it is interesting to have at one's disposal real direct in situ measurement techniques, where the concentration of nitric acid in the immediate vicinity of the instrument is derived. Few reports of such measurements are available. Profiles of the nitric acid concentration versus altitude have been obtained with the filter collection method by balloons and by aircrafts [9]. This method leads to values that are in agreement with the optical measurements, but requires long sampling times of the order of 30 min for each measuring point.

Although early attempts were made to derive in situ values for stratospheric HNO_3 mixing ratios from natural ion composition measurements [10–12], a real breakthrough was not obtained until the development of chemical ionization mass spectrometry (CIMS) by Arnold and colleagues [13].

The CIMS method, which was recently reviewed by Viggiano [14], has also been used for the detection of other minor constituents. The CIMS method is based upon the formation in a flow tube of specific product ions P^- from the reaction of stratospheric trace gases X with source ions S^- produced by an ion source from a known species. It can be easily shown [13] that the concentration of the involved trace gas $[X]$ can be derived from the equation

$$[X] = \frac{1}{k\tau} \ln\left(1 + \frac{[P^-]}{[S^-]}\right) \quad (2)$$

where the square brackets denote concentrations, k is the rate constant of the conversion of S^- into P^-, and τ is the residence time of the ions in the reaction zone. The CIMS method, originally used by Arnold and co-workers, is based upon ion molecule reactions of $CO_3^-(H_2O)_n$ and $NO_3^-(H_2O)_n$ with HNO_3 [15]. Recently, however, other reaction schemes have been developed in the laboratory and exploited for nitric acid measurements in the stratosphere and troposhere [16–19]. In the present paper we report about the use of new ion molecule reaction schemes for the measurement of HNO_3 in the stratosphere and compare the results of different methods applied simultaneously in situ.

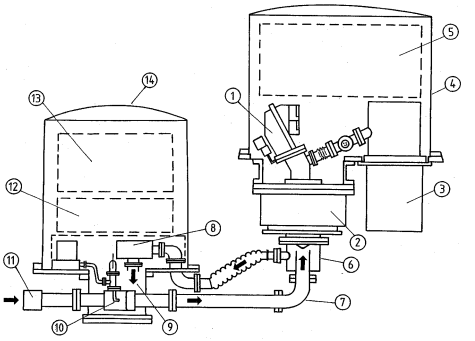

Fig. 1. Schematic representation of the MACSIMS instrument: (1) magnetic mass spectrometer; (2) and (3) cryopumps; (4) electronics container of the mass spectrometer package; (5) electronics of mass spectrometer package; (6) coupling between flow tube and mass spectrometer; (7) flow tube; (8) turbine; (9) turbine outlet connected to outside by feedthroughs in chemical ionization package container; (10) ion source block; (11) opening device (only the one at the inlet is shown, a similar one is mounted on the exit); (12) gas bottles compartment; (13) chemical ionization package electronics compartment; (14) chemical ionization package container.

2. Experiment

2.1. Instrument overview

The balloon borne instrument MACSIMS (Measurement of Atmospheric Constituents by Selective Ion Mass Spectrometry) used in this work is schematically shown in Fig. 1. It consists of three major parts: (i) an ion production package, (ii) an ion transport system, and (iii) an ion analyzer part.

The ion production package contains (a) the ion source block in which several ion sources are integrated, (b) the gas bottles with the ion source gas mixtures, (c) the valves and gas circuitry elements that control the flows of the different ion source gases

and the switching between the different ion sources, and (d) the electronics (power supplies and microprocessor) to control the ion sources. The different types of ion sources integrated in the ion source block are described later on.

The ion transport system consists of a stainless steel flow tube with an internal diameter of 3.5 cm, in which an ambient air flow is maintained by a small turbine, with a rotation frequency of 1500 Hz.

Source ions, injected into the flow tube in the ion source block at about 1 m from the ion analyzer, are transported by the ambient air flow to the mass spectrometer. On their way, part of these source ions are converted into product ions by ion molecule reactions with trace gases. If the rate constants of these ion molecule reactions are known, the concentrations of the reactive trace gases can be derived from the relative abundance of source and product ions and from the residence time of the ions in the flow tube by using Eq. (2).

The ion analyzer consists of a double focusing Mattauch–Herzog mass spectrometer [20] built in a liquid helium cryopump [21]. Ions enter the mass spectrometer through a small aperture (about 0.2 mm in diameter) in an electrically insulated inlet plate that can be biased with respect to the main structure of the instrument. For the measurement of negative ions, a voltage of +5 V is applied. The ions are guided from the inlet section to an electrostatic lens by an rf octopole lens, the axis of which is at a potential of only 0.5 V higher than the inlet plate [22]. This very low acceleration voltage in the gas expansion region just behind the ion sampling hole considerably reduces the risk for collisional breakup of cluster ions. Immediately behind the octopole an electrostatic lens accelerates the ions and focuses them into the inlet slit of the mass filter, consisting of a torroidal electrostatic and a magnetic section. In this part of the mass spectrometer, which is separately pumped by a second liquid helium cryopump, ions with different mass-to-charge ratio, accelerated to the same energy, describe different trajectories in the magnetic field sector and are focused on the image plane at different locations, forming a direct image of the mass spectrum. If we could achieve use of the full width (97 mm) of the imaging plane as a position sensitive detector, it would be possible to cover the mass range from 12 to 500 amu with only two settings of the ion acceleration voltage (IAV). However, due to the limited dimensions of commercially available photodiode arrays, two detectors, each with a span of 25.6 mm, separated by a gap of 37.3 mm, are mounted in the imaging plane. These detectors consist of a microchannel plate and a phosphor, coupled to a photodiode array by a fiber optics feedthrough [20,22]. To obtain a full spectrum, covering the whole mass range with a safe overlap, five settings of the ion acceleration voltage are required. A complete spectrum thus consists of five subspectra, each of them covering two mass ranges, corresponding to one of the two detectors and a value of the ion acceleration voltage (IAV) as shown in Table 1.

Table 1
Mass range covered by the two detectors of the mass spectrometer vs. IAV

IAV (V)	Mass range det. A (amu)	Mass range det. B (amu)
860	[17–39]	[92–144]
679	[21–51]	[118–185]
464	[32–75]	[176–274]
315	[49–113]	[264–407]
215	[74–169]	[391–587]

Ion residence times in the flow tube can be measured by pulsing the ion source and by measuring synchronously the ion current on the inlet plate with a fast electrometer. For the nominal rotation speed of 1500 Hz and for the range of pressures between 10 and 30 mb (corresponding to an altitude region of 31 to 24 km in the stratosphere), the ion residence time varies between 27 and 40 ms, depending upon the effective pumping speed of the turbine. For lower altitude, the rotation speed of the turbine decreases gradually to a value of about 1000 Hz around 60 mb, because of the increased gas load of the turbine, the power supply of which is current limited to 5 A. The associated ion residence time is regularly measured in flight.

During a balloon flight, the inlet and outlet of the flow tube are sealed off by vacuum tight covers. The

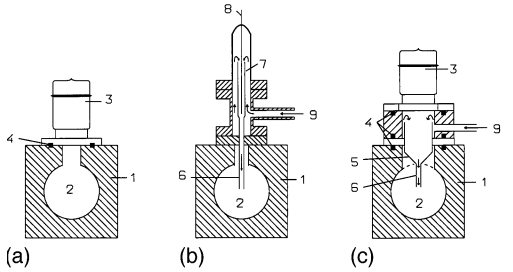

Fig. 2. (a) PEIS-CO_3^- source; (b) DIS source; (c) PEIS-CF_3O^- source: (1) ion source block; (2) flow tube cross section; (3) krypton capillary discharge lamp; (4) PTFE O-rings; (5) funnel shaped cavity illuminated by UV light and emitting photoelectrons; (6) thin wall stainless steel tube; (7) thin wall glass tube; (8) molybdenum needle molten in glass tube; (9) ion parent gas and flush gas inlet.

latter can be opened by firing pyrotechnical devices via remote control just before measurements are started, i.e. at ceiling altitude slightly above 30 km.

2.2. Ion sources

Several types of ion sources, based on different ion molecule reaction schemes, were integrated in the ion source block. Three different ion molecule reaction schemes were used for the derivation of nitric acid profiles in this work: (i) the reaction of chloride and polychloride ions with HNO_3 as discussed by Amelynck et al. [16], (ii) the conversion of CO_3^- and $CO_3^-(H_2O)_n$ ions by reaction with nitric acid [15], and (iii) the reaction of CF_3O^- with HNO_3 as recently suggested by Huey et al. [17].

2.2.1. The internal photoelectric ion source (PEIS-CO_3^-)

This photoelectric ion source (PEIS-CO_3^-), shown schematically in Fig. 2(a), produces the ions in the flow tube itself. It starts with the associative attachment of low energy electrons to neutral molecular oxygen. The electrons are produced by a small krypton discharge lamp that is mounted directly on the ion source block and that illuminates the inner metal surfaces of the flow tube with UV radiation. As a result of this, the metal wall surface emits electrons that attach very rapidly to the molecular oxygen of the ambient air to form O_2^-:

$$e^- + O_2 + M \rightarrow O_2^- + M \quad (3)$$

with a rate constant $k_3 = 3.1 \times 10^{-31} \times (300/T)^{2.5}$ cm^6 $molecule^{-2}$ s^{-1} [23] (T in K), followed immediately by

$$O_2^- + O_3 \rightarrow O_3^- + O_2 \quad (4)$$

with $k_4 = 6 \times 10^{-10}$ cm^3 $molecule^{-1}$ s^{-1} [24], and

$$O_3^- + CO_2 \rightarrow CO_3^- + O_2 \quad (5)$$

with $k_5 = 5.5 \times 10^{-10}$ cm^3 $molecule^{-1}$ s^{-1} [25]. The formation time of CO_3^- is short as compared to the residence time of the ions in the flow tube. Apart from the conversion of O_2^- by the sequence of reactions (4) and (5), formation of the hydrates $CO_3^-(H_2O)_n$ occurs either by direct hydration of CO_3^- or by a conversion scheme as described previously by Knop and Arnold [13].

2.2.2. The chlorine discharge ion source (DIS)

The discharge ion source (DIS) is schematically shown in Fig. 2(b). It consists of a small glass tube in which the ions are produced by a dc gas discharge maintained by a high voltage (1500 V) applied between an electrically insulated molybdenum needle and the circular entrance of a cylindrical stainless steel tube of 2 mm internal diameter that ends in the flow tube. The DIS can be used to make Cl_n^- (DIS-Cl mode) or I_n^- ions (DIS-I mode). For the production of Cl_n^- ions, a gas flow of a mixture of chlorine in argon (30 or 1000 ppmv) is maintained through the DIS. The major ions produced in the DIS, by using a mixture of chlorine in argon, are Cl_3^- ions and, to a lesser extent, Cl^- and Cl_2^-. Possible production mechanisms for these ions were discussed in an earlier paper [16].

The gas flow maintains in the DIS an overpressure and pushes the Cl_n^- ions formed in the discharge into the flow tube. If a gas mixture of CH_3I (methyliodide) in argon is used instead of Cl_2 in argon, I_n^- ions are produced instead of Cl_n^- ions. In this paper, however, we only discuss the results obtained with the chlorine ions.

2.2.3. The external photoelectric ion source (PEIS-CF_3O^-)

This source is used for the production of CF_3O^- ions. The reaction of these ions with HNO_3 and also with many other stratospheric trace gases, such as HCl and $ClONO_2$, results in the formation of specific product ions by fluoride transfer [17]. In this source, the principle of which is shown in Fig. 2(c), CF_3O^- ions are produced by dissociative attachment of photoelectrons, generated by illumination of the metallic surfaces of a funnel shaped stainless steel cavity with a krypton capillary discharge lamp, to bis-trifluoromethylperoxide (CF_3OOCF_3). The ion source gas is a mixture of CF_3OOCF_3 in argon ($\pm$2500 ppmv) that flows through the cavity together with a flush flow of pure argon. The ions are again pushed into the flow tube through an inlet tube with an internal diameter of 3 mm, by the overpressure existing in the ion source.

3. Results

3.1. Balloon flights

The results presented here are derived from two stratospheric balloon flights. The first balloon flight (LEON95) took place on 23 November 1995 in the CNES-INTA balloon launching base at Virgen del Camino near León (Spain, 42°35′ N, 5°38′ W).

The MACSIMS instrument weighed about 450 kg and was launched with a 100 000 m^3 valve controlled balloon at 20:18 UT (Universal Time). After having reached a ceiling altitude of 32.1 km, where the balloon was kept for about 50 min, the slow descent was started at a velocity of 1.2 m/s down to about 18 km. No technical problems occurred in flight and measurements could be made in the altitude range 32 to 18 km. As a result of the microprocessor control of the instrument and the preprogramming of the different measurement tasks in scripts, mass spectra could be recorded continuously during the balloon descent.

In this flight the instrument was equipped with two ion sources. The first one was the internal photoelectric ion source (PEIS-CO_3^-) that was used to produce CO_3^- ions and its hydrates through chemical ionization of ambient air as described in Sec. 2.2.1. The second one was a discharge ion source (DIS) where alternately Cl_n^- and I_n^- ions were produced, by sending either Cl_2 (DIS-Cl) or CH_3I (DIS-I) through the discharge. The flows of both ion source gases were kept constant, but were either sent through the DIS or evacuated to the exterior by using a pneumatic valve system. A permanent flush flow of pure argon through the DIS was maintained inbetween the switching from Cl_2 to CH_3I to remove residues of the previous ion source gas. In spite of this, the most abundant ion formed in the Ar/Cl_2 discharge became the mixed cluster ion ICl_2^- below 23 km.

The hardware for the measurement of the ion residence time in the flow tube was implemented for the first time in the LEON95 flight and has been functioning very satisfactory. Time-of-flight (TOF) spectra were obtained at 17 different altitude levels, allowing an interpolation of the TOF at intermediate altitudes to be used in the data analysis.

The second balloon flight (GAP97) took place on 17 June 1997 from the CNES launching base in Gap-Tallard in Eastern France (44°27′ N, 6°02′ E). Launching time was 20:15 UT. After an ascent of only 1 h and 5 min, the ceiling altitude of 32 km was reached at 21:20 UT. Opening devices were activated at 21:30 UT and instrument active operations were started immediately after that. The descent phase started at 23:50 UT. By using a descent velocity of about 1 m/s, measurements were performed down to about 16 km.

In this flight four ion sources were used. The PEIS-CO_3^- ion source was the same as the one used in the LEON95 flight. The DIS source, however, which was used for the alternate production of Cl_n^- and I_n^- ions in the LEON95 flight, was replaced by two separate DIS sources (one for Cl_n^- and one for I_n^- ions). The fourth ion source was the CF_3O^- source described in Sec. 2.2.3.

Only during the first part of the descent phase a measurement sequence was executed putting on all four ion sources sequentially. The majority of the data was obtained by running a shorter measurement sequence with the PEIS-CO_3^- and the PEIS-CF_3O^-

source only, because both DIS type sources have shown problems in a later stage of the flight.

3.2 Data and data analysis

3.2.1. Nitric acid derived from CO_3^- spectra

The first derivation of nitric acid concentrations in the stratosphere by Arnold and colleagues [13,15,26], based on CIMS, relied upon the reaction of the educt ions $CO_3^-(H_2O)_n$ and $NO_3^-(H_2O)_n$ with HNO_3 into product ions $CO_3^-HNO_3$ and $NO_3^-HNO_3$. The educt ions were formed in an open discharge ion source, producing the electrons required to start the reaction sequence (3), (4), and (5) to form CO_3^- followed by hydration into $CO_3^-(H_2O)_n$. This open discharge, however, also forms O_3 and NO in the flow tube, which lead to the $NO_3^-(H_2O)_n$ ions. Later on, this ion source has been replaced by a closed capillary ion source [27].

The action of our photoelectric source is assumed to be much softer than the open discharge and to produce practically only CO_3^- and $CO_3^-H_2O$ ions. The second order hydrate $CO_3^-(H_2O)_2$ is also observed, but it represents only a few percent (maximum 10% at lower altitude) of the $CO_3^-(H_2O)_n$ family. In the flow tube, CO_3^- and $CO_3^-(H_2O)_n$ are converted by the reactions,

$$CO_3^- + HNO_3 \rightarrow NO_3^- + OH + CO_2 \quad (6a)$$

$$CO_3^- + HNO_3 \rightarrow NO_3OH + CO_2 \quad (6b)$$

$$CO_3^- + HNO_3 + M \rightarrow CO_3^-HNO_3 + M \quad (6c)$$

$$CO_3^-H_2O + HNO_3 \rightarrow CO_3^-HNO_3 + H_2O \quad (7)$$

The rate constants of these reactions were determined at room temperature and at low pressure (3 mb) in the laboratory by Möhler and Arnold [15] relative to the reaction of O^- with HNO_3. As a result of a recent study of this reference reaction by Huey [28], the rate constants originally reported by Möhler and Arnold need to be corrected to $(1.6 \pm 0.6) \times 10^{-9}$ cm^3 $molecule^{-1}$ s^{-1} and $(2.0 \pm 0.5) \times 10^{-9}$ cm^3 $molecule^{-1}$ s^{-1} for reactions (6) and (7), respectively. Reaction (6) was studied recently at higher pressures (up to 18 mb) and lower temperatures (around 220 K) by Guimbaud et al. [29], who found a rate constant of $(2.4 \pm 0.7) \times 10^{-9}$ cm^3 $molecule^{-1}$ s^{-1}.

In addition, they have shown that, at the low temperatures and high pressures prevailing in the altitude range of our in situ measurements, the main channel of reaction (6) is (6c) and that the yields of the other products (NO_3^- and NO_3^-OH) are less than 10% of the total reaction products.

In all flight spectra, a series of NO_3^- core ions is observed. Their presence may also be explained by reactions of CO_3^- with trace gases other than HNO_3. Possible examples of such reactions are [30]

$$CO_3^- + NO_2 \rightarrow NO_3^- + CO_2 \quad (8)$$

$$CO_3^- + N_2O_5 \rightarrow NO_3^- + \text{products} \quad (9)$$

$$CO_3^- + ClONO_2 \rightarrow NO_3^- + ClO + CO_2 \quad (10)$$

Reactions (8) and (9) have a rate constant of 2×10^{-10} cm^3 $molecule^{-1}s^{-1}$ and 2.8×10^{-10} cm^3 $molecule^{-1}$ s^{-1}, respectively, whereas reaction (10) is occurring almost at the collision frequency (rate constant = 2.1×10^{-9} cm^3 $molecule^{-1}$ s^{-1}).

In view of the previous remarks, the following assumptions were made for the derivation of nitric acid profiles from the spectra obtained with the PEIS-CO_3^- ion source:

1. The ions CO_3^- and $CO_3^-H_2O$ are lumped together as educt ions (called R^- further on). The ion $CO_3^-(H_2O)_2$ is not considered, because it generally represents less than 10% of the $CO_3^-(H_2O)_n$ family. Its reaction with HNO_3 should give $CO_3^-HNO_3H_2O$ as product ion. The latter is only observed in small amounts (<1%);
2. All CO_3^- core ions other than $CO_3^-(H_2O)_n$ are products of the reaction of CO_3^- and $CO_3^-H_2O$ with nitric acid. The sum of these product ions will be represented by the notation $P(CO_3^-)$ hereafter;
3. Because CO_3^- and $CO_3^-H_2O$ are lumped together as educt ions and reactions (6) and (7) are proceeding with only slightly different rate constants, a common rate constant k is taken for both. The value

chosen for this common rate constant is the weighted average of the value inferred by Möhler and Arnold [15] for reaction (7) (which is expected to be only slightly temperature dependent), and the value measured at low temperature by Guimbaud et al. [29] for reaction (6);

4. All NO_3^- core ions are produced by reaction of the educt ions CO_3^- and $CO_3^-H_2O$ with trace gases other than HNO_3, called X_i hereafter. The rate constant of X_i with CO_3^- and $CO_3^-H_2O$ is k_i. The sum of the product ions is represented by $P(NO_3^-)$. Also included in this sum is $CO_3^-(H_2O)_2$, considered as the product ion of the reaction of $CO_3^-H_2O$ with the trace gas H_2O.

Neglecting ion loss by diffusion, which is playing a minimal role in the pressure range of our measurements, we can then write the following continuity equation:

$$\frac{d[R^-]}{dt} = -k[R^-]\,[HNO_3] - [R^-] \sum k_i[X_i] \quad (11)$$

which can be integrated over the residence time τ in the flow tube, leading to

$$\ln \frac{[R^-]}{[R^-]_0} = -(k[HNO_3] + \sum k_i[X_i]) \times \tau \quad (12)$$

In this formula $[R^-]_0$ is the concentration of R^- at the ion source exit. From the integration of the equations,

$$\frac{dP(CO_3^-)}{dt} = k[R^-]\,[HNO_3]$$

and

$$\frac{dP(NO_3^-)}{dt} = [R^-] \sum k_i[X_i]$$

it follows that

$$\frac{P(CO_3^-)}{P(NO_3^-)} = \frac{k[HNO_3]}{\sum k_i[X_i]}$$

Inserting this into Eq. (12) together with

$$[R^-]_0 = [R^-] + P(CO_3^-) + P(NO_3^-)$$

leads to

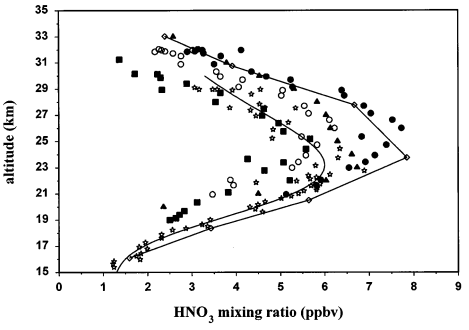

Fig. 3. Height profiles of the stratospheric nitric acid mixing ratio, obtained during the LEON95 balloon flight. Open circles: DIS-Cl (method M1), full circles: DIS-Cl (method M2), full squares: PEIS-CO_3^-, open diamonds (connected): LIMS, full triangles: Sen et al. [39], open stars: Arnold et al. [38], line: best fit through the data points of Arnold et al.

$$[HNO_3] = \frac{1}{k\tau\left(1 + \dfrac{P(NO_3^-)}{P(CO_3^-)}\right)} \times \ln\left(1 + \frac{P(CO_3^-) + P(NO_3^-)}{[R^-]}\right) \quad (13)$$

Formula (13) has been used to infer the HNO_3 profiles, shown in Figs. 3 and 4. The terms $[R^-]$, $P(NO_3^-)$, and $P(CO_3^-)$ are derived from the spectra through integration of the signal belonging to the appropriate mass peaks.

From the LEON95 balloon flight, 24 full spectra

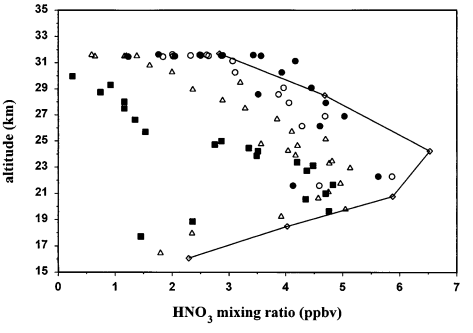

Fig. 4. Height profiles of the stratospheric nitric acid mixing ratio, obtained during the GAP97 balloon flight. Open circles: DIS-Cl (method Ml), full circles: DIS-Cl (method M2), full squares: PEIS-CO_3^-, open triangles: PEIS-CF_3O^-, open diamonds (connected): LIMS.

(each consisting of 5 subspectra) were available in the altitude range 19 to 31 km, whereas for the GAP97 flight, 21 full spectra were obtained with the PEIS-CO_3^- source on descent from 31 down to 17 km. For the LEON95 flight the major source ion observed was CO_3^- itself. Over the complete altitude range, CO_3^- represented about 60% to 65% of the $CO_3^-(H_2O)_n$ ions ($CO_3^-H_2O$ being about 30% and $CO_3^-(H_2O)_2$ less than 5%). For the GAP97 flight a similar distribution was observed down to about 25 km. At that altitude a switchover from CO_3^- to $CO_3^-H_2O$ as major source ion took place. Below 25 km the first hydrate $CO_3^-H_2O$ represented more than 70% of the source ions and the relative intensity of $CO_3^-(H_2O)_2$ increased to about 10%.

3.2.2. Nitric acid obtained with the chlorine discharge ion source

During the LEON95 balloon flight of the MAC-SIMS instrument, 26 full spectra, covering the entire mass range, were recorded on descent with the chlorine discharge ion source, from 32 to about 20 km altitude. This gave an average altitude resolution of 500 m.

During the GAP97 balloon experiment, the ion source turned out to be unstable in a later state of the flight so that the recording of useful mass spectra was limited to the altitude range 26–32 km (15 complete spectra) and to the altitude of about 22 km (2 full spectra).

In both flights two major ion families could be identified: Cl^- core ions (Cl^-, Cl^-H_2O, Cl^-HCl, Cl_2^-, and Cl_3^-) and NO_3^- core ions (NO_3^-, NO_3^-HCl, $NO_3^-H_2O$, $NO_3^-HNO_3$, $NO_3^-(HNO_3)_2$, $NO_3^-HClHNO_3$, $NO_3^-(HCl)_2$). Additionally mixed halogen ion clusters (ICl_2^- and $BrCl_2^-$) were observed. The presence of small amounts of $BrCl_2^-$ in the mass spectra was attributed to bromine contamination in the Cl_2 gas. Non-negligible concentrations of ICl_2^- ions were present in the spectra of the LEON95 balloon flight. The formation of this type of ions originated from the use of the same discharge ion source for the alternate production of polychloride and polyiodide ions and was favoured at higher pressures. Uncoupling of the polychloride and polyiodide production by using two spatially separated discharge ion sources led to the absence of the ICl_2^- ion in the GAP97 spectra. The amount of $BrCl_2^-$ ions was significantly reduced in the GAP97 flight by using a 30 ppm Cl_2 in Ar mixture instead of 1000 ppm, as in the LEON95 flight.

In both flights Cl_3^- turned out to be the most abundant source ion at all altitudes (apart from ICl_2^- below 25 km during the LEON95 flight), whereas NO_3^-HCl was always the most abundant product ion. This consideration led to a first method (M1) to derive the nitric acid concentration that only takes into account the reactions of Cl_3^- and NO_3^-HCl with HNO_3:

$$Cl_3^- + HNO_3 \rightarrow NO_3^-HCl + Cl_2 \quad (14)$$

$$NO_3^-HCl + HNO_3 \rightarrow NO_3^-HNO_3 + HCl \quad (15)$$

The rate constants of these reactions were previously measured in our laboratory flowing afterglow apparatus [16] in a relative way by using the reaction of Cl^- with HNO_3 as a reference reaction. The rate constant k_{ref} of the latter reaction was determined by several authors [28,31,32]. By using the most recent value of $(3.1 \pm 0.5) \times 10^{-9}$ cm^3 molecule^{-1} s^{-1} [32], which was found to be independent of pressure within the range 0.7–1.7 mb, and a value of 0.82 and 0.47 for k_{14}/k_{ref} and k_{15}/k_{ref}, respectively, a value of 2.6×10^{-9} cm^3 molecule^{-1} s^{-1} and 1.5×10^{-9} cm^3 molecule^{-1} s^{-1} was obtained for k_{14} and k_{15}, respectively.

Taking into account reactions (14) and (15) and assuming that (1) all Cl_3^- is formed in the ion source, (2) depletion of Cl_3^- in the flow tube is only because of the reaction with HNO_3, and (3) reaction (14) is the only source of NO_3^-HCl ions in the flow tube, $[HNO_3]$ can be obtained by the following formula:

$$[HNO_3] = \frac{1}{(k_{14} - k_{15}) \times \tau} \times \ln\left(1 + \frac{k_{14} - k_{15}}{k_{14}} \frac{[NO_3^-HCl]}{[Cl_3^-]}\right) \quad (16)$$

Part of the Cl_3^- ion production, however, is thought to take place in the flow tube itself by mechanisms involving H_2O and Cl_2 that are discussed in a com-

panion paper [32]. Therefore, the effective reaction time of the Cl_3^- ions will be smaller than the measured time of flight and the HNO_3 concentration obtained with formula (16) has to be considered as a lower limit.

A second method (M2) to derive HNO_3 concentrations with the chlorine discharge ion source is based on a global conversion of Cl^- core ions (S^-) into NO_3^- core ions (P^-). For this conversion the rate constant of HNO_3 with Cl_3^-, the most abundant source ion, is taken into account and the inferred HNO_3 concentration is given by the formula:

$$[HNO_3] = \frac{1}{k_{14}\tau} \ln\left(1 + \frac{[P^-]}{[S^-]}\right) \quad (17)$$

Laboratory measurements [32] pointed out that of all Cl^- core ions (except for Cl^-HCl, which is only present in small concentrations), the rate constant of Cl_3^- with HNO_3 is the smallest one. For this reason and also because the global conversion is partly because of reactions of the Cl^- core ions with other trace gases than HNO_3 (such as N_2O_5 and $ClONO_2$ which are present in smaller concentrations in the stratosphere compared to HNO_3), the HNO_3 concentration derived with the second method ought to be considered as an upper limit.

The HNO_3 profile obtained with both methods is shown in Figs. 3 and 4 for the LEON95 and the GAP97 flight, respectively.

3.2.3 Nitric acid derived from CF_3O^- spectra

During the GAP97 flight, the external photoelectric ion source for the production of CF_3O^- was used in situ for the first time. From the laboratory tests, performed during the development of this ion source, two source ions are expected: CF_3O^- and CF_3O^-HF, the latter being a minor source ion. Both ions were present in the flight spectra in the same relative proportion as in the laboratory test measurements. Unexpectedly, however, the flight mass spectra revealed a third and most abundant precursor ion, $CF_3O^-H_2O$, that had not been observed in the laboratory. This ion is formed in situ and presently we see different plausible explanations for its presence.

First, the three-body reaction

$$CF_3O^- + H_2O + M \rightarrow CF_3O^-H_2O + M \quad (18)$$

for which a rate constant k_{18} of 3×10^{-14} cm^3 molecule^{-1} s^{-1} was found by Huey et al. at room temperature [17], is expected to be more efficient at stratospheric temperatures. Preliminary laboratory measurements at different temperatures indeed point towards a non-negligible temperature dependence of the rate constant [33]. However, a quantitative explanation for the presence of the $CF_3O^-H_2O$ peak with water concentrations of a few ppmv as expected in the stratosphere [34] requires unrealistic high values for n, when one assumes a T^{-n} temperature dependence for the rate constant [35,36]. Further laboratory measurements are planned to clarify this point. Other conceivable explanations for the high abundance of $CF_3O^-H_2O$ are related to possible abnormally high water concentrations in the flow tube. One imaginable cause may be the outgassing of some gondola elements, leading to a locally enhanced ambient water mixing ratio. Another one may be a leak from the electronics container that is sealed at ground level before flight and that may contain air with a higher water concentration than the stratospheric air. This "wet" air could enter the flow tube through a leak in the CF_3O^- ion source, where hydration can occur. Alternatively, it can enter the flow tube through a leak in one of the other ion sources leading to the formation of $CF_3O^-H_2O$ in the flow tube itself.

Additional arguments for an abnormally high water vapour pressure come from a relatively high abundance of hydrates in the spectra obtained with the internal photoelectric ion source (PEIS-CO_3^-) in the GAP97 flight (see also Sec. 3.2.1), although no enhanced hydration was observed for the chloride ions. The latter, however, may be explained by the conversion $Cl^-H_2O + Cl_2 \rightarrow Cl_3^- + H_2O$, because this is a fast reaction [32], and chlorine is an abundant gas in the flow tube during the operation of the DIS, because of the use of Cl_2 in the ion source.

A variety of product ions is observed from the reactions of CF_3O^- and $CF_3O^-H_2O$ with HNO_3, $ClONO_2$, and HCl.

The derivation of the nitric acid profile is based on the following reaction scheme:

$$CF_3O^- + HNO_3 \rightarrow NO_3^-HF + CF_2O \quad (19)$$

with a rate constant k_{19} of 2.2×10^{-9} cm^3 $molecule^{-1}$ s^{-1} [17] and

$$CF_3O^-H_2O + HNO_3 \rightarrow CF_3O^-HNO_3 + H_2O \quad (20)$$

To our knowledge the latter reaction has not been studied yet. According to Huey et al. [17] the reaction of CF_3O^- with HNO_3 proceeds at the collision limit. Assuming that the same is true for the reaction of $CF_3O^-H_2O$ with nitric acid and taking into account that the collisional rate constants scale linearly with the inverse square of the reduced mass of the ion molecule system [37], the rate constant k_{20} is at most 5% different from k_{19}. We therefore have taken $k_{20} = k_{19}$.

The nitric acid concentration can then be inferred from the formula

$$[HNO_3] = \frac{1}{k_{19} \times \tau} \times \ln\left(1 + \frac{[P^-]}{[CF_3O^-] + [CF_3O^-H_2O]}\right) \quad (21)$$

where the family of product ions P^- consists of NO_3^-HF, $CF_3O^-HNO_3$ and the secondary reaction products $NO_3^-HFH_2O$, $CF_3O^-(HNO_3)_2$, and $NO_3^-(HNO_3)_n$ ($n = 1, 2$). The resulting nitric acid profile is shown in Fig. 4.

It should be noticed that the abovementioned source ion CF_3O^-HF has not been taken into consideration when calculating the nitric acid mixing ratio. Adding CF_3O^-HF as a third source ion in the formula causes a small shift of the calculated mixing ratio to lower values. This becomes more important at lower altitudes (below 20 km), where the CF_3O^-HF ion signal increases to more than 30% of the most abundant ion signal ($CF_3O^-H_2O$). At the present state, however, we prefer not to include CF_3O^-HF as a precursor ion, because the ion chemistry involving CF_3O^-HF remains insufficiently understood.

By taking into account the error on the time of flight and on the rate constant, as well as the reproducibility of the ratio of product to source ions, an estimated accuracy of 30% to 40% was obtained for the nitric acid mixing ratios obtained with all ion sources.

4. Discussion

An inspection of Figs. 3 and 4 reveals the following general features: (1) the magnitude of the nitric acid mixing ratios obtained with all ion sources in the altitude region 20 to 30 km is of the right order; (2) the obtained profiles have the expected form with a maximum around 24 km; (3) the mixing ratios obtained for the GAP97 flight are lower than those derived from the LEON95 data. This is in agreement with the known seasonal variation of the nitric acid distribution as inferred from the climatological data set of limb infrared monitor of the stratosphere (LIMS) [6].

The nitric acid profiles inferred from the data obtained with the chlorine discharge ion source with both methods (M1 and M2) agree within 20%. As explained in Sec. 3, the profile obtained by using method M1 should be considered as a lower limit because of the formation of Cl_3^- source ions in the flow tube itself. Moreover, the value for the rate constant of NO_3^-HCl with HNO_3 (k_{15}) has to be considered as a lower limit [16]. A more accurate determination of this rate constant could therefore result in a shift of the lower limit HNO_3 profile towards higher values.

The profile obtained by using method M2 has to be considered as an upper limit because the global conversion of Cl^- core ions to NO_3^- core ions can also partly be attributed to reaction of Cl^- core ions with trace gases other than HNO_3, such as $ClONO_2$ and N_2O_5. A good estimation of the effect of those gases on the second method requires the knowledge of the ratio of $[Cl_3^-]/[Cl^-]$ at the ion source exit, as well as the study of some additional ion molecule reactions (such as Cl_3^- with $ClONO_2$ and N_2O_5 and Cl^- with Cl_2 as a function of pressure and temperature). A better agreement between the profiles obtained with

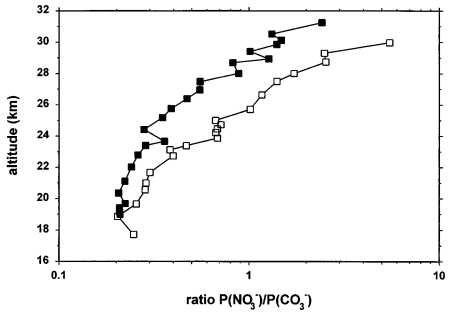

Fig. 5. Ratio of NO_3^- core product ions to CO_3^- core product ions vs. altitude. Full squares: ratio for LEON95 flight, open squares: ratio for GAP97 flight.

both methods could be obtained with an ion source producing solely Cl_3^- ions.

Below 24 km the nitric acid mixing ratios inferred from the data obtained with the PEIS-CO_3^- source are in reasonable agreement with the values derived from the other ion sources. In fact, for the LEON95 flight, the agreement with the HNO_3 mixing ratios obtained with the DIS-Cl ion source (method M1) is remarkable. Compared to the LIMS results and recently reported values [38,39], however, they are too low. Above 24 km, however, the discrepancies become more pronounced. The values obtained in the LEON95 flight are even below the lower limit obtained with the DIS-Cl (method M1).

For the GAP97 flight, the difference is even larger and a discontinuity appears around 24 km, from where (upwards on) the HNO_3 mixing ratios derived from the PEIS-CO_3^- ion source seem to be far too low. It is striking that the discontinuity of the HNO_3 profile coincides with the switchover form CO_3^- to $CO_3^-H_2O$ as major source ion. It is also worth noticing that in the GAP97 flight, the product ion ratio $P(NO_3^-)/P(CO_3^-)$ is much larger at higher altitudes than in the LEON95 flight as is illustrated in Fig. 5. A possible explanation may be a higher branching of the reaction $CO_3^- + HNO_3$ towards the products NO_3^- and NO_3OH^-. In other words, that the reaction channels (6a) and (6b), which were assumed to be negligible at stratospheric temperatures in our derivation, might have been more important in the GAP97 flight. If channels (6a) and (6b) of reaction (6), leading to NO_3^- and NO_3OH^-, would become more important, a lower value for the rate constant k should be used in formula (13). In fact, one should use $f \times k$, where f is the fractional reaction probability for the three-body channel (6c) of (6).

Möhler and Arnold [15] reported an abundance of about 60% for the product ions NO_3^- and NO_3OH^- from a laboratory study of reaction (6) at room temperature and at a pressure of 3 mb. This would correspond to a value for f of 0.4. However, in a more recent study at higher pressure (12 mb) and also at room temperature, Guimbaud et al. [29] found for the abundance of NO_3^- and NO_3OH^- about 40%, corresponding to a value of 0.6 for *f*, whereas for a temperature of 212 ± 5 K and pressures above 6 mb a value of 0.85 for f was reported by these authors.

Because the temperature above 24 km in the GAP97 flight was only slightly higher compared to the LEON95 flight (a difference of the order of 6 K was observed above 25 km), the foregoing explanation would require an extremely strong temperature dependence of the branching ratio of reaction (6), which seems to be contradictory to the existing experimental laboratory data. It is clear, however, that in order to refine the derivation of nitric acid concentrations from the CO_3^- spectra and to validate the assumptions used in Sec. 3.2.1., careful laboratory measurements of the reaction $CO_3^- + HNO_3$ and the product distribution as a function of pressure and temperature must be performed.

Apart from the error induced by the uncertainty on the rate constant, another error source is existing. Because not all ion intensities were determined at the same ion acceleration voltage in flight, a correction factor has to be applied on some ion signals to account for the transmission dependence of the ion acceleration voltage (IAV). This correction plays an important role for the spectra obtained with the CO_3^- source, whereas for the other ion sources most of the major ions were recorded on the same IAV and application of the IAV correction does not have a large impact on the obtained mixing ratios. This correction factor, which is derived from the flight data by using the signals of ions that are recorded on different IAV values, induces another supplementary error that may

partly explain the differences in the HNO_3 data derived from the CO_3^- spectra and those from other ion sources.

The HNO_3 mixing ratio profile derived from the spectra obtained with the CF_3O^- ion source in the GAP97 flight is, within the accuracy of the measurements, in reasonable agreement with the other profiles shown. Only at higher altitudes, there is a small tendency to somewhat lower values.

During this flight, the usefulness of this ion source for measuring HNO_3 mixing ratios in the stratosphere has been demonstrated. Moreover, because of the selectivity of product ion formation in the reactions of CF_3O^- with other trace gases, like HCl and $ClONO_2$, the use of this ion source for simultaneous measurements of different trace gases looks very promising. Optimisation is, however, necessary and additional laboratory measurements are needed to fully understand the reactions involving CF_3O^- and $CF_3O^-H_2O$ to explain the large abundance of the hydrated ion $CF_3O^-H_2O$ in the spectra and to investigate the possible role of the source ion CF_3O^-HF.

5. Conclusions

Stratospheric nitric acid concentrations have been derived by CIMS based upon different ion molecule reaction schemes. Apart from the results obtained with the PEIS-CO_3^- source above 24 km in the last balloon flight, there is, within the error bars, a reasonable agreement between the mixing ratios obtained by the different methods.

The chlorine discharge ion source allows the derivation of an upper and lower limit for the nitric acid mixing ratio. The use of Cl_3^- as a source ion looks very attractive, because this ion reacts selectively with HNO_3 to form NO_3^-HCl, whereas the reaction products (or a fraction of them) of Cl^- and CO_3^- with HNO_3 are NO_3^- ions, which can also result from the reaction with other nitrogen containing trace gases, such as N_2O_5 and $ClONO_2$. Optimisation of the DIS-Cl ion source leading to production of Cl_3^- only, instead of Cl^- and Cl_3^-, should lead to one single profile instead of an upper and lower limit.

As far as the PEIS-CO_3^- is concerned, it is believed at present that a better knowledge of the branching ratio as a function of temperature of the reaction of CO_3^- with nitric acid is required to interpret the data recorded with this ion source. The use of the CF_3O^- source looks very promising, especially because of the selectivity of product ion formation in the reactions of CF_3O^- with other trace gases like HCl and $ClONO_2$ that should allow simultaneous measurements of different trace gases.

Acknowledgements

The authors would like to thank the following for their support: the Commission of the European Communities (contract nos. EV5V-CT92-0062 and ENV4-CT95-0042), the FKFO/MI (Fonds voor Kollektief Fundamenteel Onderzoek-Ministerieel Initiatief), the CNES (Centre National d'Etudes Spatiales, France), and the SNF (Schweizerischer Nationalfonds zur Förderung der wissenschaftlichen Forschung und Bundesamt für Bildung und Wissenschaft). One of us (C.A.) gratefully acknowledges support by the Belgische Staat, Diensten van de Eerste Minister-Federale diensten voor wetenschappelijke, technische en culturele aangelegenheden and another one (C.G.) by the Conseil Regional du Centre. The authors are also indebted to the CNES launching team and the INTA representatives for their excellent collaboration during the balloon flight campaigns and to Professor H. Willner for the preparation of the CF_3OOCF_3.

References

[1] J.B. Burkholder, P.D. Hammer, C.J. Howard, J. Phys. Chem. 91 (1987) 2136.
[2] World Meterological Organization, Global Ozone Research and Monitoring Project, Report No. 16, "Atmospheric Ozone 1985, Assessment of our understanding of the processes controlling its present distribution and change" (and references therein), Vol. II, 1985.
[3] P.J. Crutzen, Quart. J. Met. Soc. 96 (1970) 320.
[4] World Meterological Organization, Global Ozone Research and Monitoring Project, Report No. 37, "Scientific Assessment of Ozone Depletion: 1994" (and references therein), 1994.

[5] M.M. Abbas, V.G. Kunde, J.C. Brasunas, J.R. Herman, S.T. Masie, J. Geophys. Res. 96 (1991) 10,885.
[6] J.C. Gille, P.L. Bailey, C.A. Graig, Adv. Space Res. 18(9/10) (1996) 125.
[7] J.B. Kumer, J.L. Mergenthaler, A.E. Roche, R.W. Nightingale, G.A. Ely, W.G. Uplinger, J.C. Gille, S.T. Massie, P.L. Bailey, M.R. Gunson, M.C. Abrams, G.C. Toon, B. sen, J.-F. Blavier, R.A. Stachnik, C.R. Webster, R.D. May, D.G. Murcray, F.J. Murcray, A. Goldman, W.A. Traub, K.W. Jucks, D.G. Johnson, J. Geophys. Res. 101 (1996) 9621.
[8] H. Schlager, F. Arnold, D. Hofmann, T. Deshler, Geophys. Res. Lett. 17 (1990) 1275.
[9] A.L. Lazrus, B.W. Ganrud, J. Atmos. Sci. 31 (1974) 1102.
[10] F. Arnold, R. Fabian, G. Henschen, W. Joos, Planet. Space Sci. 28 (1980) 681.
[11] A.A. Viggiano, F. Arnold, Planet. Space. Sci. 29 (1981) 895.
[12] E. Arijs, D. Nevejans, J. Ingels, Adv. Space Res. 4 (1984) 19.
[13] G. Knop, F. Arnold, Planet. Space. Sci. 33 (1985) 983.
[14] A.A. Viggiano, Mass Spectrom. Rev. 12 (1993) 115.
[15] O. Möhler, F. Arnold, J. Atmos. Chem. 13 (1991) 33.
[16] C. Amelynck, D. Fussen, E. Arijs, Int. J. Mass Spectrom. Ion Proceedings 133 (1994) 13.
[17] L.G. Huey, P.W. Villata, E.J. Dunlea, D.R. Hanson, C.J. Howard, J. Phys. Chem. 100 (1996) 190.
[18] L.G. Huey, and E.R. Lovejoy, Int. J. Mass Spectrom. Ion Proceedings 155 (1996) 133.
[19] R.L. Mauldin III, D.J. Tanner, F.L. Eisele, J. Geophys. Res. 103 (1998) 3361.
[20] R. Moor, E. Kopp, U. Jenzer, H. Ramseyer, U. Wälchli, E. Arijs, D. Nevejans, J. Ingels, D. Fussen, A. Barassin, C. Reynaud, in Proceedings of the Ninth ESA/PAC Symposium on “European Rocket and Ballon Programmes and Related Research,” Lahnstein, FRG, 3–7 April 1989 (ESA SP-291 June 1989).
[21] J. Ingels, E. Arijs, D. Nevejans, D. Forth, G. Schaeffer, Rev. Sci. Instrum. 49 (1978) 782.
[22] C. Rytz, E. Kopp, P. Eberhardt, Int. J. Mass Spectrom. Ion Processes 137 (1994) 155.
[23] G. Brasseur, S. Solomon, Aeronomy of the Middle Atmosphere, 2nd ed., Reidel, Dordrecht, 1986.
[24] D.W. Fahey, H. Böhringer, F.C. Fehsenfeld, E.E. Ferguson, J. Chem. Phys. 76 (1982) 1801.
[25] I. Dotan, J.A. Davidson, G.E. Streit, D.L. Albritton, F.C. Fehsenfeld, J. Chem. Phys. 67 (1977) 2874.
[26] F. Arnold, G. Knop, Int. J. Mass Spectrom. Ion Processes 81 (1987) 33.
[27] O. Möhler, T. Reiner, F. Arnold, Rev. Sci. Instrum. 64 (1993) 1199.
[28] L. G. Huey, Int. J. Mass Spectrom. Ion Processes 153 (1996) 153.
[29] C. Guimbaud, D. Labonnette, V. Catoire, R. Thomas, Int. J. Mass Spectrom. 178 (1998) 161–171.
[30] Y. Ikezoe, S. Matsuoka, M. Takebe, A.A. Viggiano, Gas Phase Ion-Molecule Reaction Rate Constants Through 1986, Maruto, Tokyo, 1987.
[31] F.C. Fehsenfeld, C.J. Howard, A.L. Schmeltekopf, J. Chem. Phys. 63 (1975) 2835.
[32] C. Amelynck, E. Arijs, N. Schoon, A.-M. Van Bavel, Int. J. Mass Spectrom. 181 (1998) 113.
[33] C. Guimbaud, D. Labonnette, V. Catoire, unpublished results.
[34] M.M. Abbas, H.A. Michelsen, M.R. Gunson, M.C. Abrams, M.J. Newchurch, R.J. Salawitch, A.Y. Chang, A. Goldman, F.W. Irion, G.L. Manney, E.J. Moyer, R. Nagaraju, C.P. Rinsland, G.P. Stiller, R. Zander, Geophys. Res. Lett. 23 (1996) 2401.
[35] A.A. Viggiano, J. Chem. Phys. 81 (1984) 2639.
[36] A.A. Viggiano, J. Chem. Phys. 84 (1986) 244.
[37] T. Su, M.T. Bowers, Gas Phase Ion Chemistry, Vol. 1, M.T. Bowers (Ed.), Academic, New York, 1979, Chap. 3.
[38] F. Arnold, K. Gollinger, S. Spreng, in Polar Stratospheric Ozone, J.A. Pyle, N.R.P. Harris and G.T. Amanatidis (Eds.), Air Pollution Report 56, 175–178, European Commission, Brussels, 1996.
[39] B. Sen, G.C. Toon, G.B. Osterman, J.-F. Blavier, J.J. Margitan, R.J. Salawitch, G.K. Yue, J. Geophys. Res. 103 (1998) 3771.